

Supporting Information

Performance-limiting Formation Kinetics in Green Water-Processed Perovskite Solar Cells

Peng Zhai^{a*}, Lixia Ren^{a*}, Yanrui Zhang^a, Zhuo Xu^a, Yin Wu^a, Kui Zhao^a, Lu Zhang^a, Shengzhong (Frank) Liu^{a,b,*}

^aKey Laboratory for Applied Surface and Colloid Chemistry, National Ministry of Education; Shaanxi Engineering Lab for Advanced Energy Technology; School of Materials Science and Engineering, Shaanxi Normal University, Xi'an 710119, China.

^bDalian Institute of Chemical Physics, Chinese Academy of Sciences, Dalian, 116023, China; Center of Materials Science and Optoelectronics Engineering, University of Chinese Academy of Sciences, Beijing 100049, P. R. China.

Correspondence: zhaipeng@snnu.edu.cn; renlixia@snnu.edu.cn; szliu@dicp.ac.cn

Experimental section

Materials

Pb(NO₃)₂ (> 99%), Pb(HCOO)₂ (> 99%), Pb(SCN)₂ (> 99%) and PbCO₃ (> 99%) were purchased from Sigma-Aldrich. Formamidinium iodide (FAI), methylammonium iodide (MAI), methylammonium chloride (MACl) and *n*-octylammonium iodide (OAI) were purchased from Xi'an Polymer Light Technology Corp.

Device fabrication

Fluoride-doped tin oxide glass substrate was sequentially cleaned by 2% commercial detergent water solution, deionized water, ethanol and acetone in ultrasonic bath for 15 min, rinsed with deionized water and then dried by air blowgun. After O₃/ultraviolet treatment for 15 min, the 40 nm compact layer TiO₂ (c-TiO₂) was deposited on a cleaned FTO substrate by chemical bath method. The mesoporous TiO₂ (mp-TiO₂) was spin-coated at 4000 rpm for 20 s onto the c-TiO₂ using a commercial paste (Greatcell 30 NR-D) diluted in ethanol (1:6, weight ratio) to achieve 150 to 200 nm thickness. After drying at 80 °C for 10 min, the TiO₂ films were gradually sintered to 500 °C, kept at this temperature for 30 min and cooled to room temperature. Before use, the films were treated with Li₂CO₃ aqueous solution (1 mg/mL) by spin coating at 3000 rpm for 20 s and then were sintered at 450 °C for 30 min. After cooling down to room temperature and O₃/ultraviolet treatment for 15 min, the substrates were transferred to dry-air glovebox (relative humidity < 10%) for deposition of perovskite films. Pure aqueous Pb(NO₃)₂ solution (1.5 M) was prepared by adding Pb(NO₃)₂ into DI water, followed by sonicating for 1 hour to form the stable solution. Halide-free lead NFs were prepared by adding insoluble lead salts into an aqueous Pb(NO₃)₂ solution. 5 mg Pb(HCOO)₂ and Pb(SCN)₂, and 2 mg PbCO₃ were incorporated in 1 mL Pb(NO₃)₂ solution (1.5 M), respectively. Excessive introduction will result in precipitation, while too little introduction will result in dissolution. These precursors were sonicated for 1 hour to form the stable suspensions and then were spin coated onto the substrate at 5000 rpm for 20 s, and dried at 70 °C on a hot plate for 30 min. After cooling to room temperature, the Pb(NO₃)₂-infiltrated mesoporous TiO₂ film was immersed in an IPA solution containing MAX (MAI/MACl = 4:1) with the concentration of around 10 mg/mL. The total incubation time was split into 3 sectors. For instance, the total dipping time for PbCO₃ was 6 min, in which the first cycle lasted 4 min and the other two cycles needed 1 min for each. After the conversion of Pb(NO₃)₂ to MAPbI_{3-x}Cl_x is completed, a

solution of FAI: MAI: MACl (25mg: 2.5mg: 2.5mg in 1ml IPA) was spin-coated atop the MAPbI_{3-x}Cl_x layer at a spin rate of 2000 rpm for 30 s, followed by annealing at 150 °C for 10 min to obtain FA-rich perovskite film. Upon cooling to room temperature, OAI solution (4 mg/mL in IPA) was spin coated on the perovskite at 5000 rpm for 30 s, followed by 100 °C for 10 min. The spiro-OMeTAD layer was spin-coated onto the perovskite films. Finally, an 80-nm-thick gold electrode was thermally evaporated onto the stack.

Thin films characterizations

For in situ PL measurement, a homebuilt platform consists of a 405-nm laser diode and an Ocean Optics Spectrometer (Flame) coupled with optical fibers and several planoconvex lenses. Surface morphology images of the perovskite films or PSC devices were obtained using a field emission scanning electron microscope (Jeol SU-8020). X-ray diffraction (XRD) patterns were acquired using a Bruker D8 GADDS diffractometer with the Cu K α radiation. CV measurements (CHI660E) were carried out in a 3-electrode configuration using an Ag/AgCl, KCl (saturated) reference electrode, a Pt wire as the counter electrode and the PbI₂ film as the working electrode in a 0.38 M 1-ethyl-3-methylimidazolium bis(trifluoromethylsulfonyl)imide (EMIm TFSI) in IPA solution. In the TEM characterization, the film was scratched off from the substrate and then dispersed in hexane; it was treated with ultrasound for 10 min before dropping on a copper grid. The XPS measurements were performed in a VG ESCALAB MK2 system with monochromatized Al K α radiation at a pressure of 5.0×10^{-7} Pa. The absorption spectra of the annealed perovskite films were obtained by a Shimadzu UV-3600 spectrophotometer. Samples were excited using a continuous-wave laser (OBIS LX, 660 nm) whose power was adjusted to match the photogeneration rate under one Sun illumination (0.324 mW, 0.786 mm effective beam FWHM). The signal was collected using an integrating sphere (Gigahertz Optik, UPB-150-ARTA) connected via a multimode, 400 mm diameter optical fiber (Thorlabs BFL44LS01) to a spectrometer (Andor, Kymera 193i). The system was spectrally calibrated using an irradiance calibration standard lamp (Gigahertz Optik, BN-LH250-V01). Absolute photoluminescence measurements were performed with a 520 nm continuous-wave laser (Insaneware) whose power was adjusted to match the photogeneration rate under one Sun illumination. The signal was collected using an integrating sphere connected via a multimode, 400 mm diameter optical fiber (Thorlabs BFL44LS01) to a spectrometer (Andor, Kymera 193i). The system was spectrally

calibrated using an irradiance calibration standard lamp. The TAS measurements were performed at various power densities (from 2.98 to 14.90 $\mu\text{J}/\text{cm}^2$). The femtosecond laser pulse was generated by a Ti:sapphire femtosecond regenerative amplifier with 500 nm wavelength and 50 kHz repetition rate (Coherence) and served as both pump and probe beams. The spot size of the TA is approximately 0.008 mm^2 as evaluated by imaging the laser spot. All experiments were carried out at room temperature (i.e., $T=300\text{ K}$).

Device measurements

Before measurement, a non-reflective metal mask with aperture area (0.0812 cm^2) was covered on the top of the device (0.10 cm^2) to precisely define the active area and ensure that no illumination or voltage biasing condition had been introduced. The current-voltage (IV) scan was recorded with a computer-controlled digital source meter (Keithley 2400) under exposure of a solar simulator (XES-40S2-CE, Class AAA, San-Ei Electric, AM 1.5G filter at 100 mW cm^{-2}). The light intensity of 1 Sun illumination was calibrated using a Si-reference cell (the 91150V model, Newport, UK). The voltage scan rate was 50 mV s^{-1} in forward and reverse scans under ambient conditions (25 $^\circ\text{C}$, relative humidity $\sim 40\%$). For indoor light test, the data was recorded using a Keithley 2400 Source Meter under a warm-white 2700 K LED light (DYSON, CD05, 2700 K) illumination. EQE spectra of PSCs were measured using a Q Test Station 500TI system (Crowntech, Inc. USA). The monochromatic light intensity was adjusted using a reference silicon detector. In the light intensity dependent V_{OC} examination, the light intensity was controlled using an ND filter (Shibuya Optical Co., LTD, Japan) that covered the top of the device. All photovoltaic parameters were extracted from the average IV curve of forward (from short-circuit to open-circuit) and reverse (from open-circuit to short-circuit) scans. For the light soaking stability test, unencapsulated PSCs with UV-filter were placed in a N_2 -filled glove box under one sun irradiation at the open circuit condition. The chamber atmosphere temperature is controlled at $30\pm 5\text{ }^\circ\text{C}$.

DFT calculations

In this work, the density-functional theory (DFT) calculations were performed using the Vienna Ab initio Simulation Package (VASP). The projected augmented wave (PAW) method and the Perdew-Burke-Ernzerhof (PBE) exchange-correlation functional within the generalized gradient approximation (GGA) were used to obtain the lattice constants. An energy cutoff of 500 eV was

set for the plane-wave function's expansion. The van der Waals (vdW) dispersion correction was found necessary to yield more accurate lattice constants, which are described by the DFT-D3 correction. The primitive unit cell structures of cubic-phase FAPbI₃ are first obtained by applying Monkhorst-Pack sampling with a Γ -centered $5\times 5\times 5$ k-point grid. Slabs models are constructed on a $3\times 3\times 1$ supercell with thickness of seven layers for FAI-terminal surface. The slabs are separated by a vacuum spacing >15 Å to avoid the interaction between period slabs with the top three layer fully relaxed. Then Brillouin zone of FAPbI₃[001] slabs are sampled by a $1\times 1\times 1$ k-mesh. In all geometric optimization, the residual force was converged until the total energy changes were less than 1.0×10^{-5} eV and the maximum force component acting on each atom was less than 0.05 eV Å⁻¹.

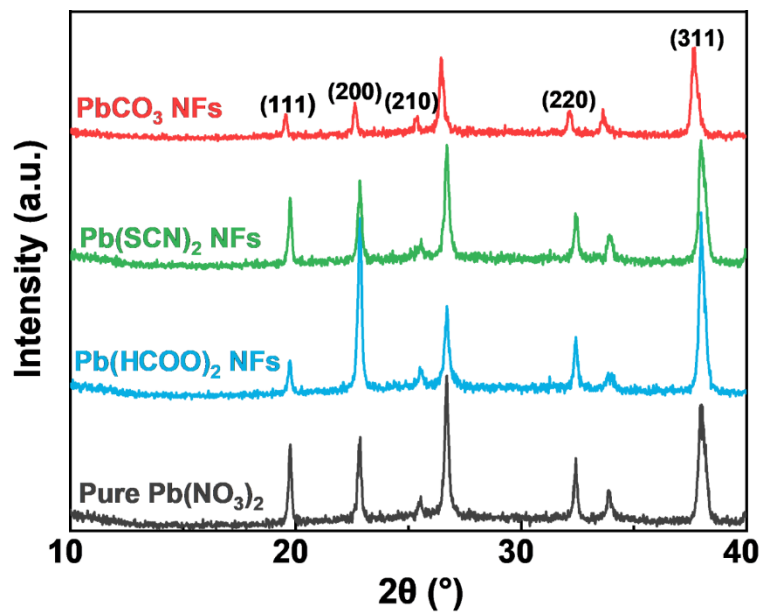


Figure S1 XRD spectra of Pb(NO₃)₂ films prepared from various NFs.

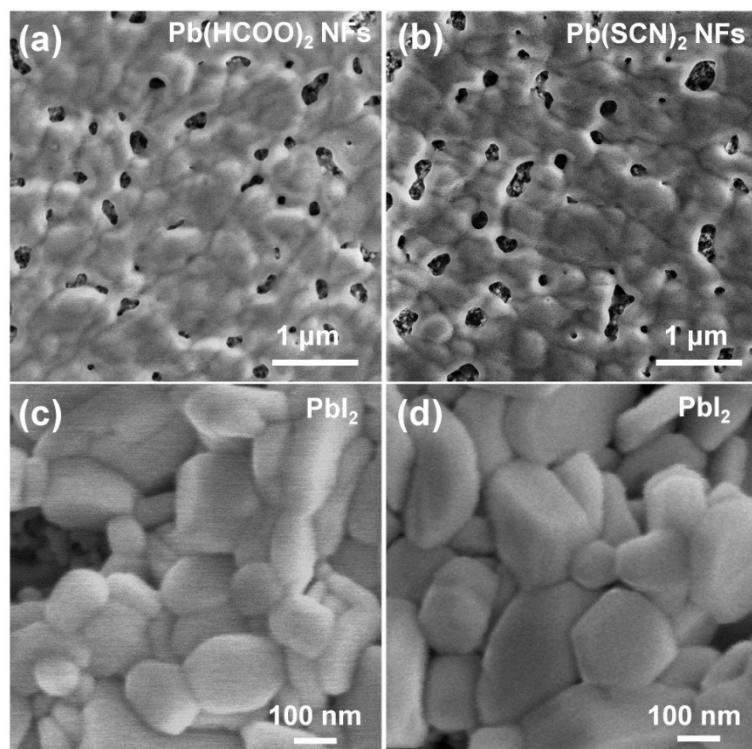


Figure S2 SEM images of the $\text{Pb}(\text{NO}_3)_2$ films and their created PbI_2 films. (a-b) $\text{Pb}(\text{NO}_3)_2$ films prepared from $\text{Pb}(\text{HCOO})_2$ and $\text{Pb}(\text{SCN})_2$ NFs and (c-d) the refined PbI_2 crystals.

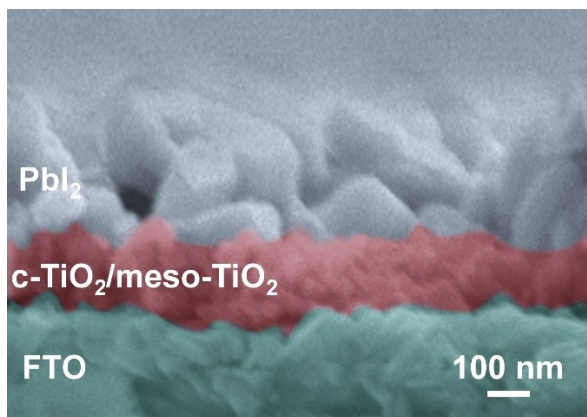


Figure S3 Cross-sectional images of the newly transformed PbI_2 film.

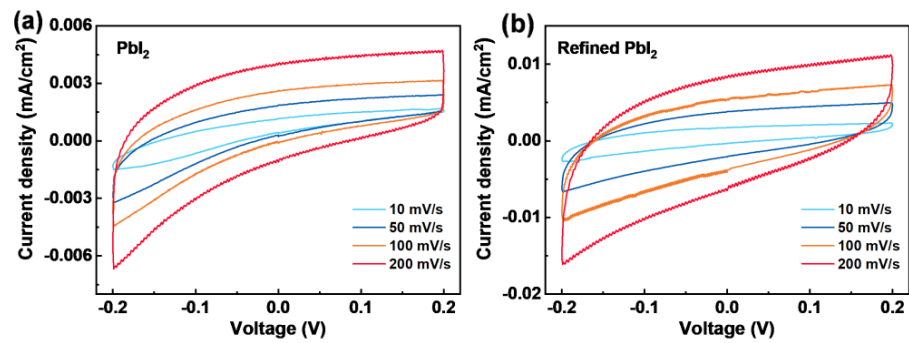


Figure S4 CV curves of PbI₂ films at different scan rates ranging from 10 to 200 mV/s in an ionic liquid.

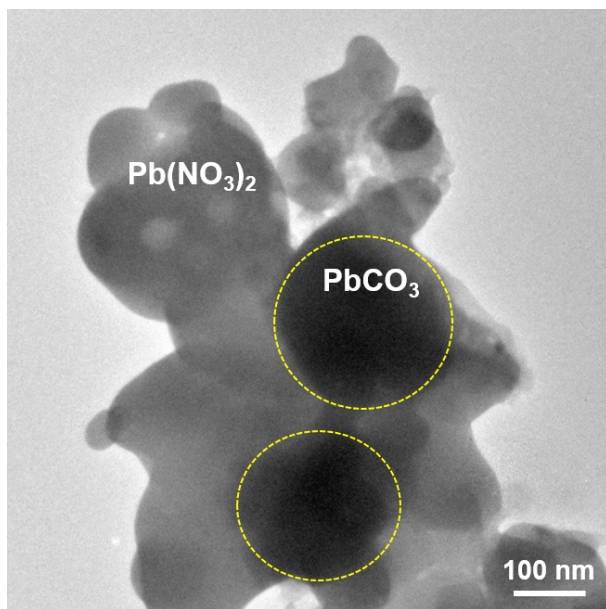


Figure S5 TEM image of PbCO_3 NFs sample.

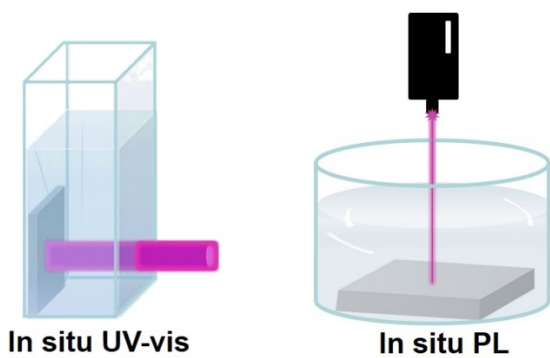


Figure S6 Illustration of the in situ UV-Vis absorption/PL measurements during incubation.

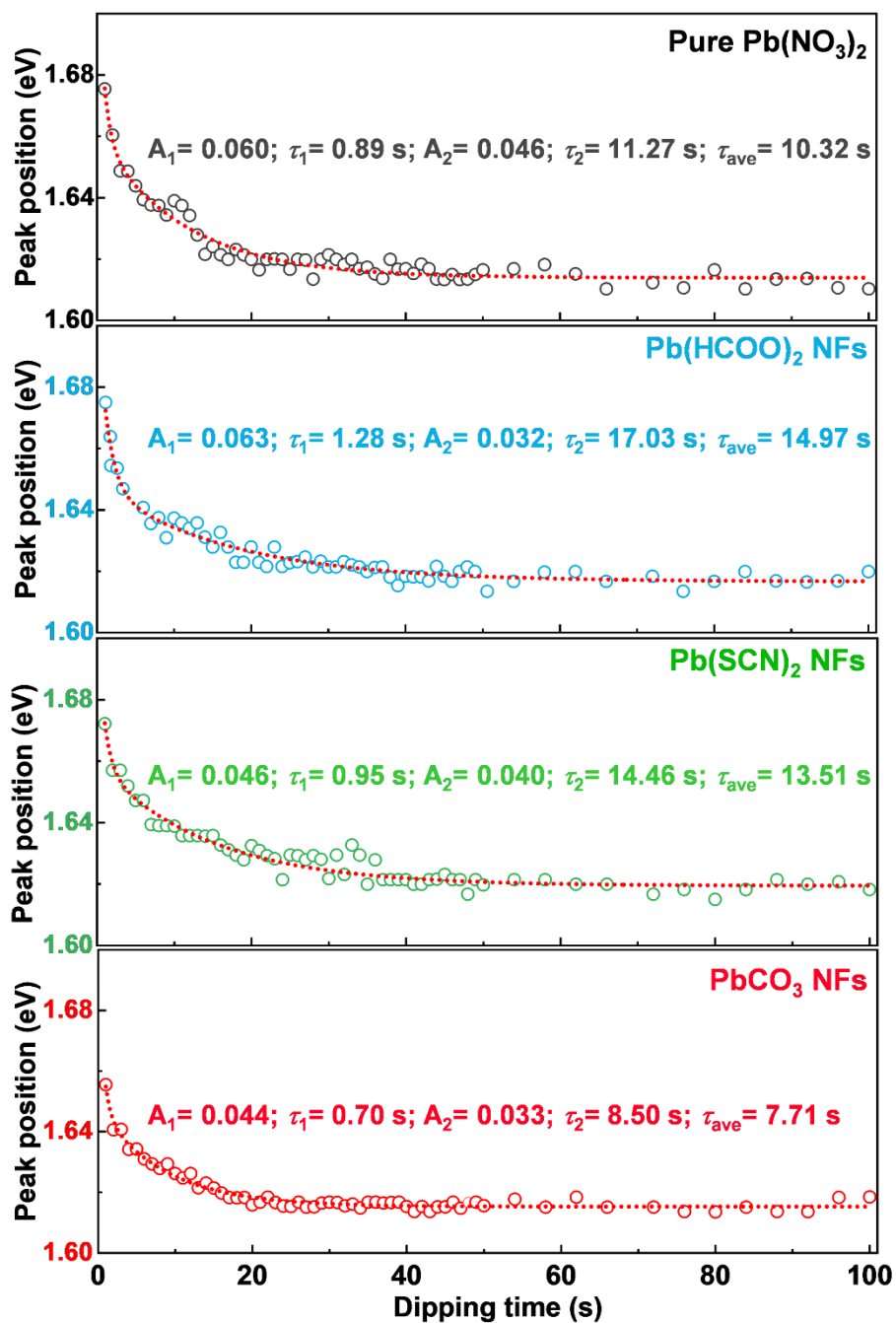


Figure S7 The extracted values of emission peak position. By fitting the peak position signals during incubation with a bi-exponential decay model, it is found that PbCO_3 NFs accelerate the time to reach the target stoichiometry.

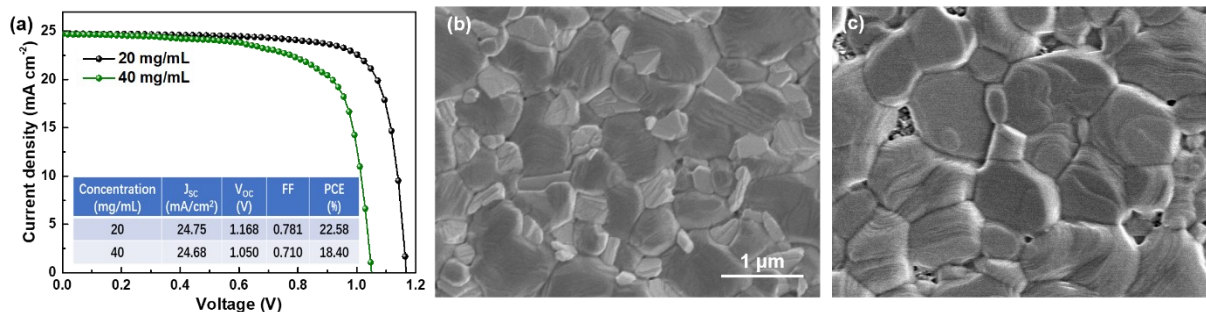


Figure S8 J-V curves of PbCO_3 NFs based PSCs prepared with different post-dripping concentrations; SEM image of perovskite film prepared with (b) 20 mg/mL and (c) 40 mg/mL post-dripping solution.

Different solution concentrations are investigated and 30 mg/mL is proved to be the optimal (shown in Fig. 4b). PCEs based on these perovskites are shown in Fig. S8a. At a low concentration (20 mg/mL), PbI_2 particles are mostly distributed at grain boundaries (in Fig. S8b) where perovskites are prone to decomposition, because the insufficient FA-MA intermixing results in poor thermal stability. Excessive PbI_2 adversely affect the charge collection at the interface, resulting in FF lower than the target PSCs (30 mg/mL). At higher concentration (40 mg/mL), the excess amount of I⁻ from the post-dripping solution may dissolve the initially formed $\text{MAPbI}_{3-x}\text{Cl}_x$ layer, leading to pin hole defects on the surface (in Fig. S8c).

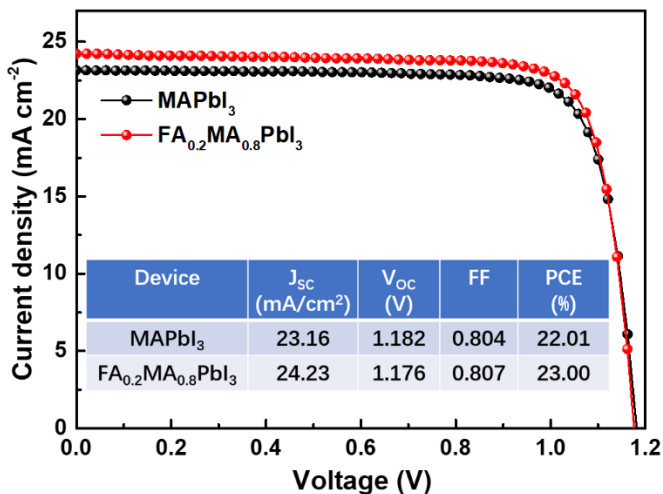


Figure S9 J-V curves of PbCO₃ NFs based PSCs prepared with different FA-MA composition.

To confirm the universality of this preparation method, MA-rich perovskite (FA_{0.2}MA_{0.8}PbI₃) and MAPbI₃ are prepared by using PbCO₃ NFs. A post-dripping solution of FAI: MAI = 1:4 (molar ratio) or pure MAI were spin-coated atop the MAPbI_{3-x}Cl_x layer, respectively. The concentration is controlled at 30 mg/mL.

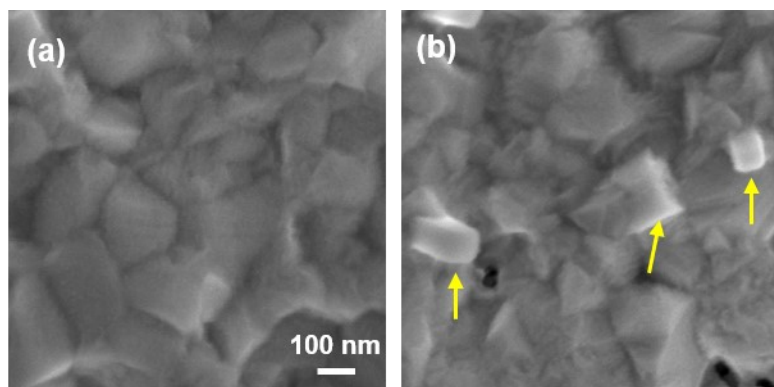


Figure S10 SEM images of the unannealed $\text{MAPbI}_{3-x}\text{Cl}_x$ films. (a) $\text{MAPbI}_{3-x}\text{Cl}_x$ prepared from PbCO_3 NFs, the dipping time is 6 min; and (b) $\text{MAPbI}_{3-x}\text{Cl}_x$ prepared from $\text{Pb}(\text{HCOO})_2$ NFs, the dipping time is 12 min. The yellow arrow refers to the perovskite cuboids induced by the Ostwald ripening effect.

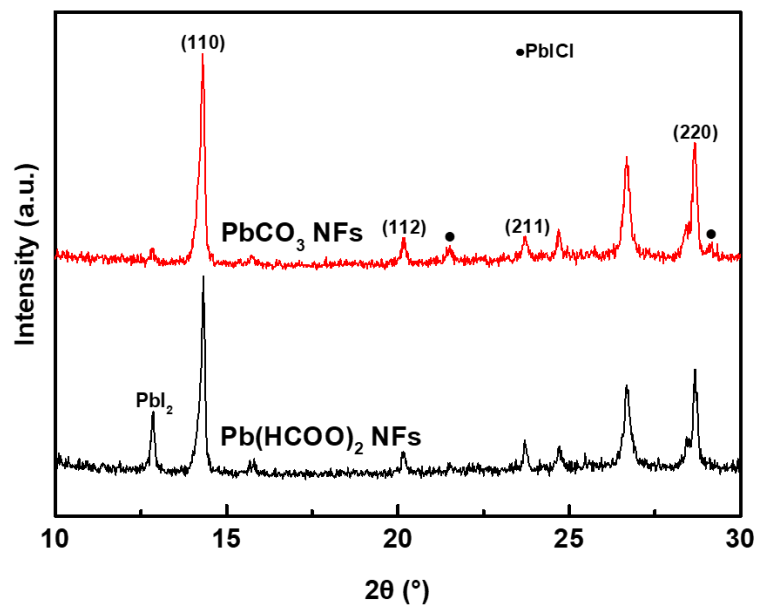


Figure S11 XRD spectra of $\text{MAPbI}_{3-x}\text{Cl}_x$ films prepared from Pb(HCOO)_2 and PbCO_3 NFs without annealing.



Figure S12 Digital image of various lead salts.

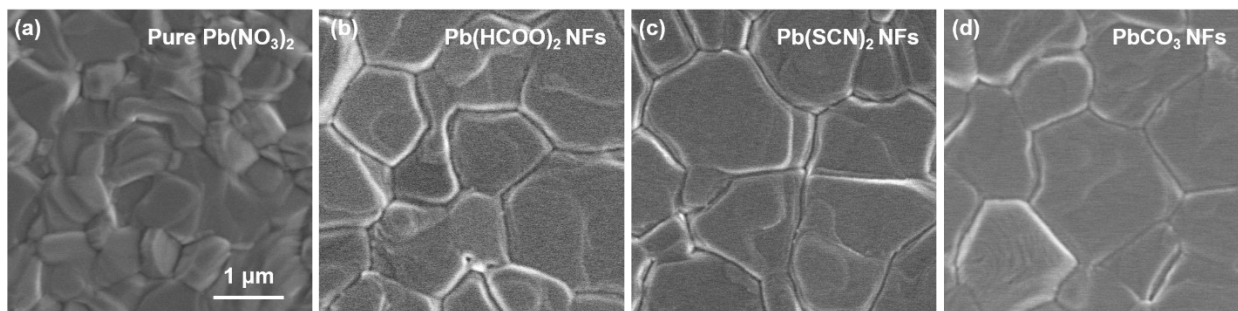


Figure S13 SEM images of the resultant perovskite films. (a) perovskite prepared from the pure $\text{Pb}(\text{NO}_3)_2$; (b-d) perovskites prepared from the $\text{Pb}(\text{HCOO})_2$, $\text{Pb}(\text{SCN})_2$ and PbCO_3 NFs, respectively.

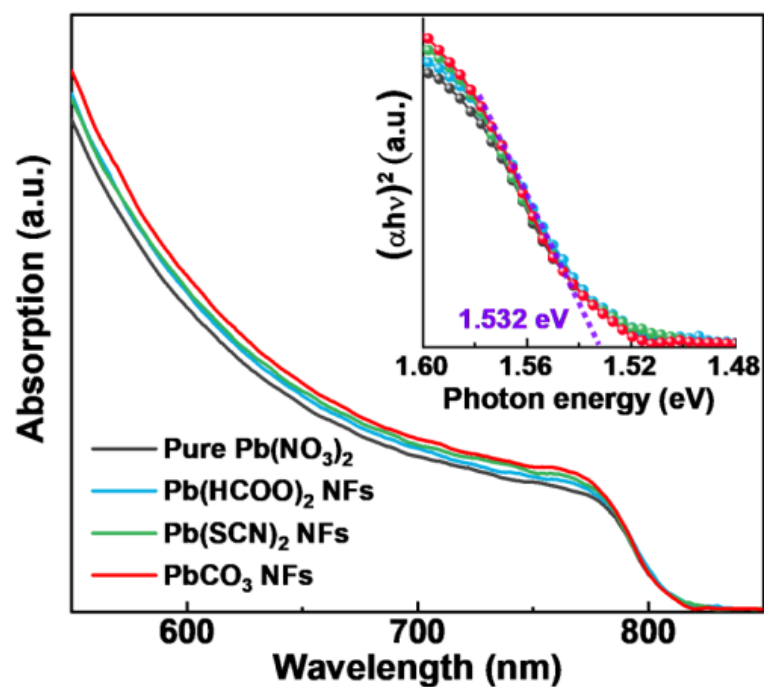


Figure S14 Absorbance spectra of the perovskite films processed using different $\text{Pb}(\text{NO}_3)_2$ substrates.

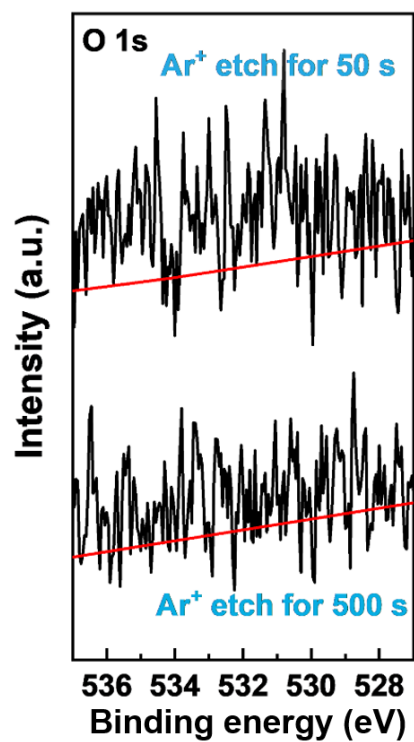


Figure S15 Narrow scanning XPS spectra of O 1s. The sample was etched using the Ar⁺ plasma for 50 s and 500 s.

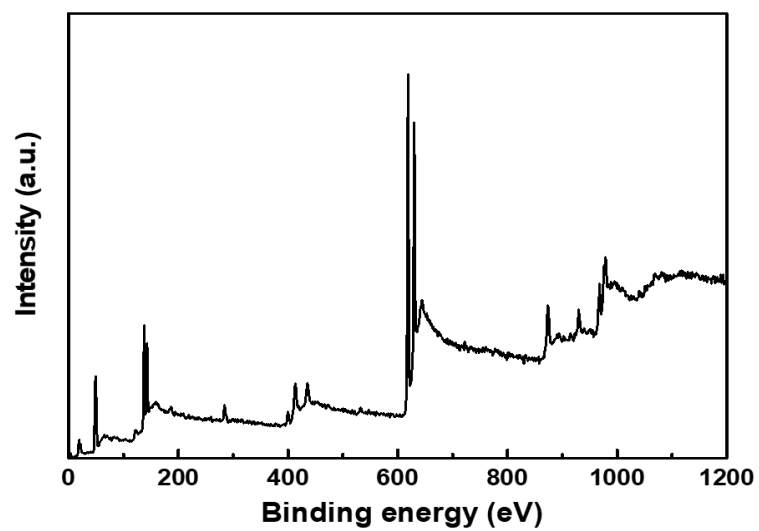


Figure S16 The surface composition of perovskite film. XPS full scan of the reference perovskite film, Pb $4f$ and I $3d$ peaks were integrated to determine the surface composition.

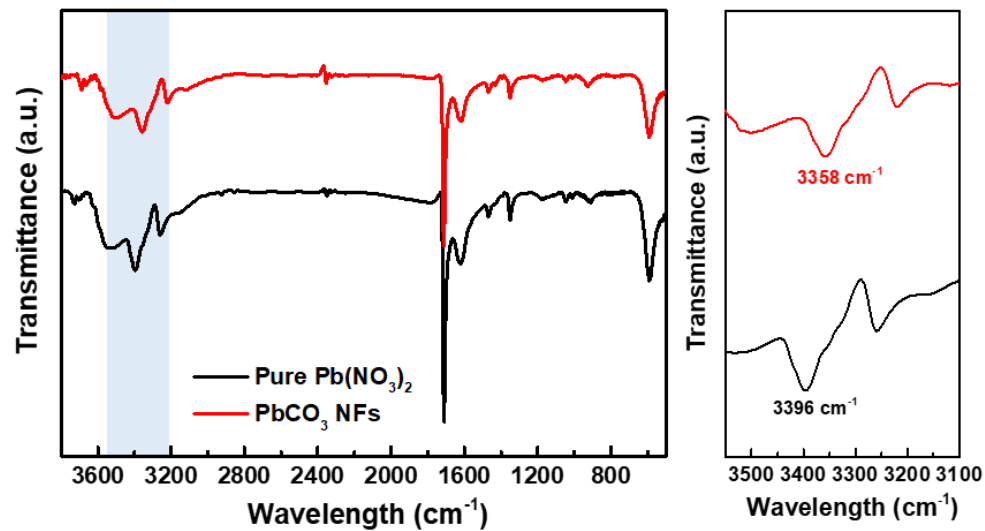


Figure S17 The interaction between FA⁺ and CO₃²⁻ unveiled by FTIR vibrational spectroscopy. The proposed hydrogen bonding between CO₃²⁻ and FA resulted in a shift in FA vibrational peaks (N-H stretch near 3400 cm⁻¹).

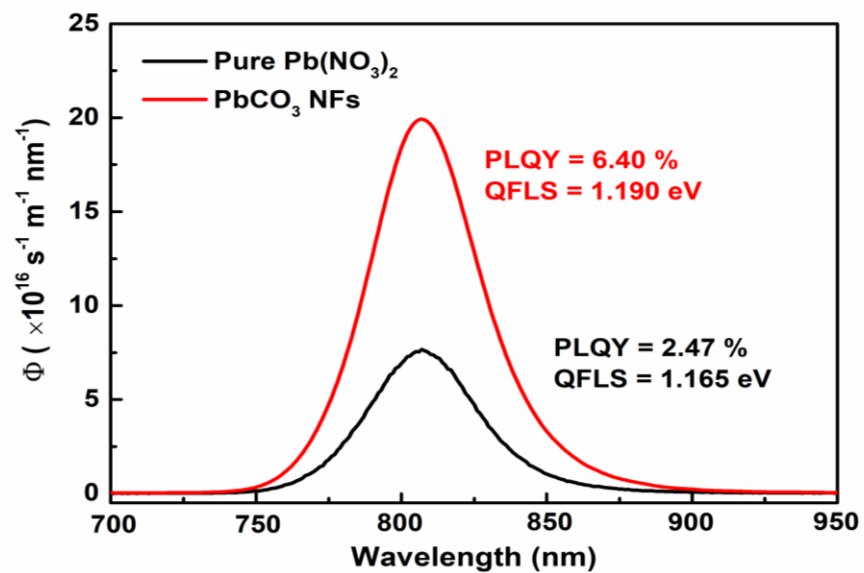


Figure S18 Photoluminescence spectra photon flux Φ of the perovskite films. a.u., arbitrary units.

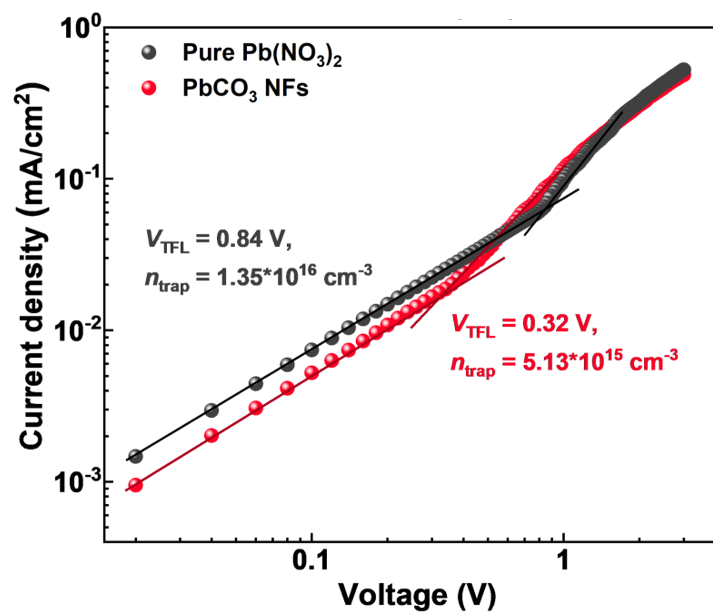


Figure S19 Space-charge-limited current (SCLC) curves of devices with an electron-only FTO/c-TiO₂/mp-TiO₂/perovskite/PCBM/Ag structure.

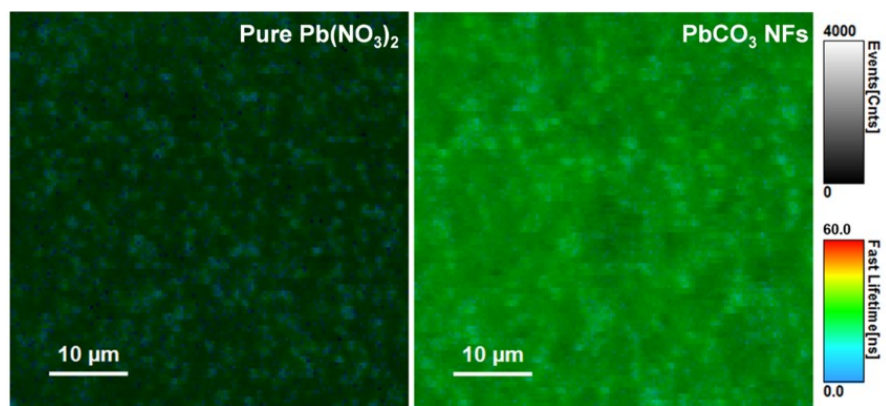


Figure S20 2D PL mapping of the perovskite films prepared from pure Pb(NO₃)₂ and PbCO₃ NFs.

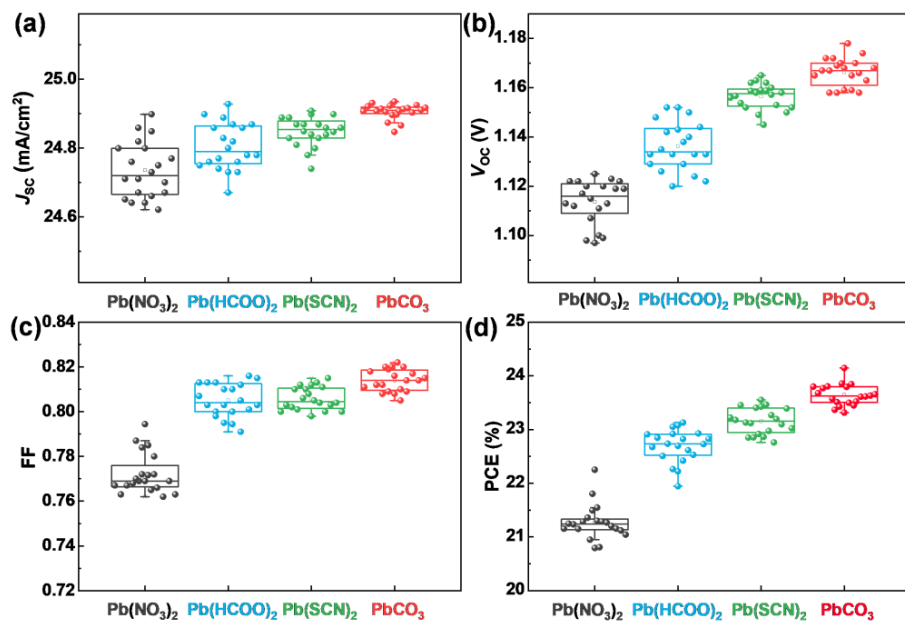


Figure S21 Statistical distribution diagram of the devices. (a)-(d) Box plots of I-V characteristics of PSCs made with different perovskite. All data are statistical results of 20 devices made from different batches.

Scan direction	Test items	Unit	Test conditions & requirements	Test results
Forward scan	V _{oc}	V	a. The tested device is unencapsulated and tested under the ambient conditions (25 °C and RH ~35 %); b. Aperture area: 0.088 cm ² ; c. By using the standard solar cell to calibrate the solar simulator's irradiance to 100 mW/cm ² ;	1.142
	J _{sc}	mA/cm ²		25.79
	Fill factor	%		76.45
	Efficiency	%		22.52
Reverse scan	V _{oc}	V	d. Scan Direction: reverse 1.2V to -0.1V, forward -0.1V to 1.2V; Stepping: 0.02 V; Delay time: 100 ms	1.148
	J _{sc}	mA/cm ²		25.81
	Fill factor	%		78.83
	Efficiency	%		23.36

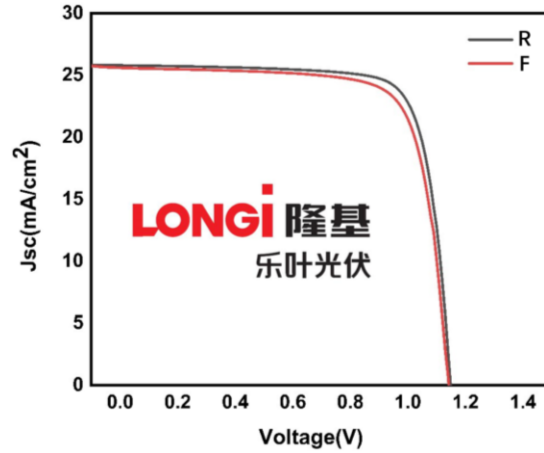


Figure S22 Test report from the world's leading photovoltaic company (LONGi).

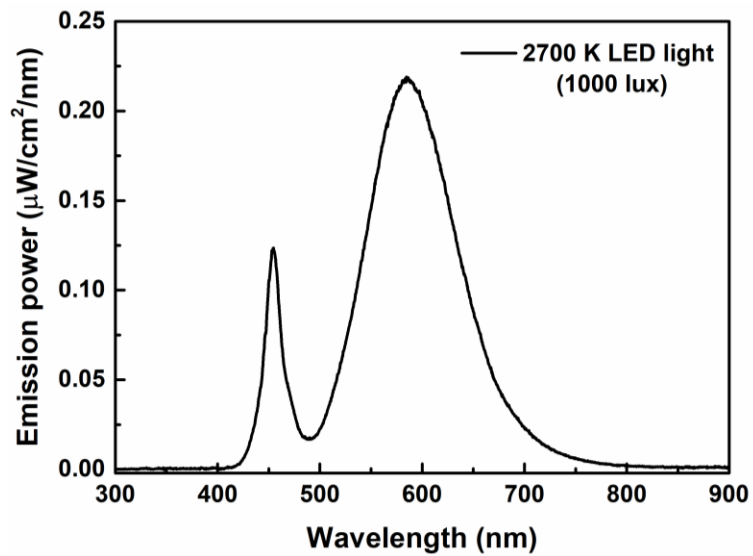


Figure S23 Emission power and integrated power spectra of the white 2700 K LED normalized to 1000 lux.

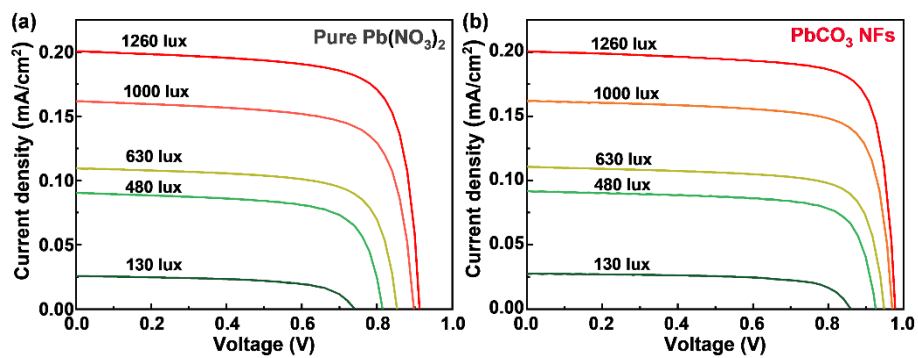


Figure S24 Indoor J-V curves of the PSCs prepared from (a) pure Pb(NO₃)₂ and (b) PbCO₃ NFs under different LED light illumination.

Table S1. Photovoltaic parameter deviation of the PSCs prepared from pure Pb(NO₃)₂ and various NFs.

Device	V_{OC} (V)	J_{SC} (mA cm ⁻²)	FF (%)	PCE (%)
Pure Pb(NO ₃) ₂	1.114 ± 0.009	24.74 ± 0.082	77.22 ± 0.902	21.27 ± 0.328
Pb(HCOO) ₂ NFs	1.136 ± 0.010	24.80 ± 0.068	80.51 ± 0.744	22.69 ± 0.307
Pb(SCN) ₂ NFs	1.156 ± 0.010	24.85 ± 0.043	80.59 ± 0.514	23.16 ± 0.240
PbCO ₃ NFs	1.166 ± 0.006	24.91 ± 0.022	81.40 ± 0.494	23.64 ± 0.200

Table S2. Summary of the photovoltaic parameters for the best pure Pb(NO₃)₂ and PbCO₃ NFs based PSCs.

Devices	Scan direction	V_{oc} (V)	J_{sc} (mA/cm ²)	FF	PCE (%)	HI (%)
Pure Pb(NO ₃) ₂	Forward	1.111	24.85	0.772	21.31	4.2
	Reverse	1.125	24.91	0.794	22.25	
PbCO ₃ NFs	Forward	1.170	24.93	0.816	23.80	1.5
	Reverse	1.178	24.95	0.822	24.16	

Table S3. Photovoltaic parameters of the PSCs under 2700 K LED light source with different light intensities.

Devices	Light intensity (lux)	P_{in} ($\mu\text{W}/\text{cm}^2$)	J_{sc} ($\mu\text{A}/\text{cm}^2$)	V_{oc} (V)	FF	P_{out} ($\mu\text{W}/\text{cm}^2$)	PCE (%) ^a
Pure $\text{Pb}(\text{NO}_3)_2$	1260	384.6	200.37	0.913	0.749	137.0	35.6
	1000	305.2	161.67	0.898	0.729	105.8	34.7
	630	193.8	109.62	0.853	0.714	66.8	34.5
	480	152.3	90.43	0.815	0.696	51.3	33.7
	130	39.8	25.70	0.741	0.616	11.7	29.4
PbCO_3 NFs	1260	384.6	200.49	0.978	0.785	153.9	40.0
	1000	305.2	161.71	0.970	0.771	120.9	39.6
	630	193.8	110.76	0.938	0.749	77.8	40.1
	480	152.3	91.82	0.926	0.735	62.5	41.0
	130	39.8	27.31	0.860	0.670	15.7	39.4

^aThe PCEs are averaged from more than 10 independent cells. The PCE of all the photovoltaic cells is defined and calculated according to the following equation: $\text{PCE} = P_{out}/P_{in} \times 100\%$.

Table S4. Summary of fitting parameters of fluence-dependent normalized TA kinetic traces for the perovskite films.

Sample	Pump fluence ($\mu\text{J}/\text{cm}^2$)	τ_1 (ps)	Intensity A_1 (%)	τ_2 (ns)	Intensity A_2 (%)	τ_{ave} (ns)
Pure $\text{Pb}(\text{NO}_3)_2$	2.98	1.302	0.504	3.124	0.496	3.122
	5.96	1.321	0.429	2.766	0.571	2.765
	11.92	1.312	0.395	2.640	0.605	2.639
	14.90	1.351	0.354	2.494	0.646	2.493
PbCO ₃ NFs	2.98	2.897	0.543	3.522	0.457	3.518
	5.96	2.999	0.490	3.305	0.510	3.302
	11.92	2.893	0.366	3.197	0.634	3.196
	14.90	3.335	0.338	2.729	0.662	2.727